Bilayer Nanotubes and Helical Ribbons Formed by Hydrated Galactosylceramides: Acyl Chain and Headgroup Effects

Vitthal S. Kulkarni, Wayne H. Anderson, and Rhoderick E. Brown
The Hormel Institute, University of Minnesota, Austin, Minnesota 55912-3698 USA

ABSTRACT The molecular basis of bilayer tubule formation in hydrated galactosylceramide (GalCer) dispersions has been investigated by synthesizing different chain-pure GalCers and examining their aqueous mesomorphic phase structure by freeze fracture and negative-stain electron microscopy. Thermotropic characterization of the GalCer species by differential scanning calorimetry provided supplementary information that verified the phase state under which morphological observations were carried out. Under aqueous conditions and at room temperature, *N*-24:1$^{\Delta 15(cis)}$ GalSph, the predominant monounsaturated, nonhydroxy acyl species of bovine brain GalCer (NFA-GalCer), formed cylindrical mesomorphic self-assemblies consisting almost exclusively of "nanotubes," i.e., lipid bilayer tubules of relatively uniform length and diameter (length, 250–400 nm; diameter, 25–30 nm). In contrast, N-24:0 GalSph, the major saturated, nonhydroxy acyl species of bovine brain GalCer, displayed no tendency to form these relatively small "nanotubes." Rather, N-24:0 GalSph formed larger, variable-length ribbon-like structures (length, 5,000–10,000 nm) that often appeared to undulate and, occasionally, appeared to be helically twisted. Interestingly, bovine brain GalCer, which contains high levels of the N-24:1$^{\Delta 15(cis)}$ and N-24:0 species as well as 2-hydroxy acyl chains, formed multilamellar liposomes of variable size and showed little tendency to form cylindrical structures. This result suggested that changes to the polar interface/headgroup region imparted by the 2-hydroxy acyl species strongly influenced bilayer tubule and cylinder formation in GalCer. To define this influence more clearly, other sphingoid-based and glycerol-based lipids were investigated. Morphological characterization of N-24:1$^{\Delta 15(cis)}$ sphingosylphosphorylcholine (24:1 SM) revealed no evidence of bilayer cylinder or tubule formation. Similar results were obtained with aqueous dispersions of 1-palmitoyl-2-nervonoyl phosphatidylcholine (16:0, 24:1 PC). Hence, the bulkier, more hydrated, zwitterionic phosphocholine headgroup inhibited the formation of bilayer nanotubes and cylinders under physiological saline conditions.

INTRODUCTION

Renewed interest in lipid self-assembly has been driven, in part, by attempts to engineer lipid templates for the production of rugged, stable nano- and microstructures by metallization and mineralization processes (Yager et al., 1992; Archibald and Mann, 1993; Schnur, 1993; Schnur et al., 1994). As a result, a variety of lipid amphiphiles have been identified that spontaneously form tubular bilayer mesophases. Synthetic lipids that display such tendencies include certain two-chain ammonium amphiphiles (Nakashima et al., 1985) as well as phosphatidylcholines with hydrocarbon chains containing diacetylenic functional groups (Schnur et al., 1987, 1994; Rudolph et al., 1991; Schoen et al., 1993). However, lipid tubule and cylinder formation is not confined to synthetic lipids but also has been reported for various biological lipids (Lin et al., 1982; Mishima et al., 1992; Kodama et al., 1993). In fact, it has been suggested that if naturally occurring lipids could be used to replace diacetylenic lipids, the applications costs could be reduced substantially (Yager et al., 1992). Among the most striking examples of biological lipids that form bilayer tubules and cochleate myelinic cylinders are monoglycosylated sphingolipids. These lipids, commonly known as cerebrosides (see Fig. 1), are minor components of most cell membranes, with the exception of specialized membranes like intestinal brush border and the myelin sheaths of the central and peripheral nervous systems (O'Brien and Sampson, 1965; Svennerholm et al., 1992). The relatively high cerebroside levels in myelin are thought to be necessary for maintaining the unusually low proton permeability of myelin lipid bilayers (Díaz and Monreal, 1994). However, in the inherited pathological conditions known as Gaucher's and Krabbe's diseases, cerebrosides accumulate excessively, disrupt normal membrane function, and form intracellular lipid deposits (Naito et al., 1988). In the case of Krabbe's disease, also known as globoid cell leukodystrophy, it is the cerebroside, galactosylceramide (GalCer), that accumulates in excess and, in doing so, gives rise to helical tubules and ribbon-like structures within afflicted cells (Yunis and Lee, 1970).

Received for publication 26 May 1995 and in final form 31 July 1995.

Address reprint requests to Dr. Rhoderick E. Brown, The Hormel Institute, University of Minnesota, 801 16th Avenue NE, Austin, MN 55912. Tel.: 507-437-9625; Fax: 507-437-9606; E-mail: reb@maroon.tc.umn.edu.

Portions of this investigation were presented at the FASEB Summer Conference on Membrane Molecular Biophysics: Structure and Function held at Saxtons River, VT on July 16–20, 1994, and at the 39th Annual Meeting of the Biophysical Society held at San Francisco on February 12–16, 1995.

Abbreviations used: GalCer, galactosylceramide; N-acyl GalSph, *N*-acyl galactosyl sphingosine; GalSpd, deacylated GalCer with naturally occurring sphingoid base composition, usually sphingosine (= 90%) and dihydrosphingosine (= 10%); N-acyl SPC, *N*-acyl sphingosylphosphorylcholine; SM, sphingomyelin; PNPC, 1-palmitoyl-2-nervonoyl phosphatidylcholine; TLC, thin-layer chromatography; EM, electron microscopy; DSC, differential scanning calorimetry.

0006-3495/95/11/1976/00 $2.00

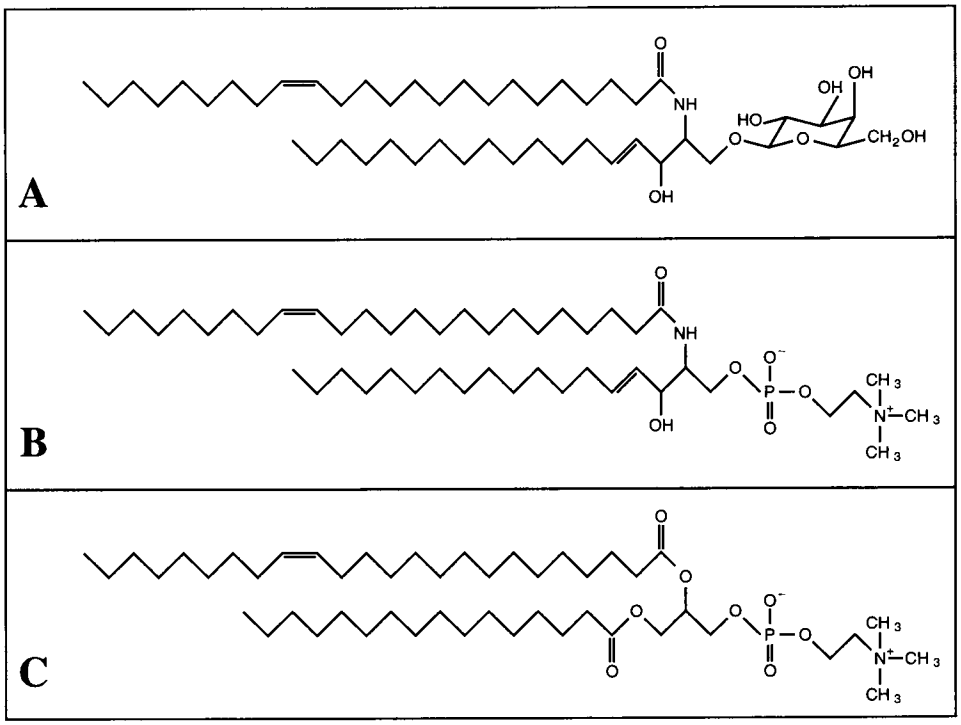

FIGURE 1 Configurations of structurally similar galactosylceramide, phosphatidylcholine, and sphingomyelin. (*A*) Galactosylceramide containing a nervonoyl ($24:1^{\Delta 15(c)}$) acyl chain representing the major unsaturated NFA-GalCer species found in bovine brain. (*B*) Sphingomyelin containing a nervonoyl acyl chain. (*C*) 1-palmitoyl-2-nervonoyl phosphatidylcholine (PNPC).

The unusual physical properties of GalCer (compared to glycerol-based phospholipids) are well documented (for reviews, see Koynova and Caffrey, 1995; Maggio, 1994; Curatolo, 1987; Thompson and Tillack, 1985). Although hydrated dispersions of GalCer form lamellar bilayer assemblies (e.g., Pascher and Sundell, 1977; Reed and Shipley, 1987), this monoglycosylated sphingolipid has the capacity to form extraordinarily stable lamellar crystalline phases (Bunow, 1979; Curatolo, 1982; Curatolo and Jungalwala, 1985; Lee et al., 1986). Interestingly, alteration of GalCer's acyl chain length (e.g., palmitate (16:0), stearate (18:0), or lignocerate (24:0)) has little effect on the high enthalpy, lamellar crystal-to-liquid crystal phase transition temperature that occurs near 82°C (Ruocco et al., 1983; Curatolo and Jungalwala, 1985; Reed and Shipley, 1987). However, introduction of *cis* unsaturation strongly affects GalCer's bilayer (Reed and Shipley, 1989) and monolayer phase behavior (Ali et al., 1991, 1993, 1994). Key factors thought to contribute to GalCer's unusual physical properties include the ability to form hydrogen bonds (e.g., Bunow and Levin, 1980; Pink et al., 1988) and a naturally occurring acyl composition with mostly very long, saturated fatty acids and very long, saturated, 2-hydroxy fatty acids (e.g., Johnson and Brown, 1992). In fact, based on FT-IR data, various metastable, gel-like phases have been reported in bovine brain GalCer, providing the possibility for the coexistence of multiple lateral domains enriched in various GalCer species (Jackson et al., 1988). Also, among sulfated GalCer species, acyl chain length asymmetry is believed to result in stable, mixed interdigitated, gel phases for long acyl chain species and metastable, partially interdigitated gel phases for shorter acyl chain species (Boggs et al., 1988b).

Recent attempts to understand how the acyl composition of GalCer affects its mesomorphic phase structure have focused on bovine brain GalCer or its subfractions, all of which contain a heterogeneous array of nonhydroxy acyl chains (NFA-GalCer) or 2-hydroxy acyl chains (HFA-GalCer) (e.g., Archibald and Yager, 1992; Archibald and Mann, 1993, 1994). In cases where these GalCer subfractions formed lipid bilayer tubules, high levels of nonaqueous solvents were needed to produce the desired mesomorphic assembly. However, as alluded to above, GalCer inclusions often take the form of helical tubules and ribbon-like structures in cells afflicted with globoid cell leukodystrophy (Yunis and Lee, 1970). Hence, what remains unclear is which, if any, of the individual molecular species known to be present in naturally occurring bovine brain GalCer form lipid bilayer tubules when placed in an aqueous environment.

Here, we have investigated the molecular basis of tubule formation in hydrated GalCer dispersions by synthesizing different chain-pure GalCers, which are major components of naturally occurring GalCer, and investigating their mesomorphic features by freeze fracture and negative-stain electron microscopy. We complemented the morphological studies by thermotropic characterization of the GalCer species using differential scanning calorimetry. Our results indicate that the presence of nervonoyl ($24:1^{\Delta 15(c)}$) acyl residues in GalCer promotes the formation of "nanotubes." The presence of lignoceroyl (24:0) acyl residues in GalCer results in larger undulating, ribbon-like structures that appear to be helically twisted. By comparing our GalCer

results to those obtained with structurally similar sphingomyelins and phosphatidylcholines (Fig. 1), we found that the bulkier, more hydrated, zwitterionic phosphorylcholine headgroup inhibited bilayer tubule and ribbon formation under physiological saline conditions.

MATERIALS AND METHODS

Synthesis of homogeneously N-acylated GalSph

Bovine brain GalCer (Avanti Polar Lipids, Alabaster, AL) was deacylated by alkaline hydrolysis to obtain galactosylsphingoid (GalSpd or psychosine) (Radin, 1974). Purification of the galactosylsphingosine (GalSph) fraction was achieved by medium-pressure flash column chromatography on silica gel (230–400 mesh) using step gradients consisting of $CHCl_3$/CH_3OH (85:15) and CH_3OH/iso-$CH_3CH_2CH_2OH$/2.5 M NH_4OH (10:65:25). The absence of the dihydro fraction of psychosine was confirmed by thin-layer chromatography (TLC) using $CHCl_3/CH_3OH/H_2O/NH_4OH$ (70:30:4:1) as the solvent system (Radin, 1974). The *N*-hydroxy succinimide ester derivatives of desired fatty acids were prepared (Lapidot et al., 1967) and then reacted with GalSph in the presence of the catalyst, *N*-ethyldiisopropylamine, at 60°C under nitrogen for 4 h (Schwarzmann and Sandhoff, 1987) to obtain homogeneously N-acylated GalSph. The reaction product (N-acylated GalSph) was purified either by flash column chromatography on 230–400-mesh silica gel column using solvent system $CHCl_3$/CH_3OH/H_2O (90:10:0.5) or by preparative TLC on silica gel GF 1000 μ plates. Silica gel that coeluted with the lipid was removed by Folch partitioning (Kates, 1986). Recrystallization of the lipid was achieved by dissolving in a minimal amount of hot $CHCl_3/CH_3OH$ (4:1), precipitating with cold acetone (−20°C), and collecting the precipitated lipid by low-speed centrifugation at 4°C. The final product was freed of remaining traces of silica gel by suspending in hexane/isopropanol (7:2) and centrifuging at 4°C to pellet the insoluble silica gel. By following this procedure, we prepared *N*-lignoceroyl galactosylsphingosine (N-24:0 GalSph) and *N*-nervonoyl galactosylsphingosine (N-24:$1^{\Delta 15(c)}$ GalSph). Concentrations of stock solutions (dissolved in hexane/isopropanol/water, 70/30/2.5 v/v) were determined by dry weight on a Cahn microbalance (model 4700).

Synthesis of *N*-nervonoyl-sphingomyelin

Egg sphingomyelin (Avanti Polar Lipids) was deacylated by hydrolyzing in methanolic HCl at 65–75°C for about 36 h (Cohen et al., 1984). The reaction product, sphingosylphosphorylcholine (lyso-sphingomyelin, SPC), was purified by flash column chromatography and recrystallized. Reacylation of the lyso SM was achieved by reacting with the *N*-hydroxy succinimide ester of nervonic acid (24:$1^{\Delta 15(c)}$) in 5% aqueous $NaHCO_3$/ethanol (9:1, v/v; pH 8) while refluxing at 90°C for 4 h (Ahmad et al., 1985). The mixture was cooled and adjusted to pH 3 by adding an appropriate amount of 1 M HCl. Precipitated lipid (including SM) was pelleted by low-speed centrifugation, and the aqueous phase was extracted for remaining SM with theoretical lower Folch phase ($CHCl_3/CH_3OH/H_2O$: 88/12/0.6) (Kates, 1986). The crude SM was purified by flash column chromatography on 230–400 mesh silica gel using a step-gradient solvent system consisting of $CHCl_3/CH_3OH$ (85:15) and $CHCl_3/CH_3OH/H_2O$ (55:45:10). The final product, *N*-nervonoyl SM (N-24:$1^{\Delta 15(c)}$ SPC), was recrystallized and freed from traces of silica gel by the same procedure as described for GalCer derivatives. The final stock concentration of *N*-nervonoyl SM, determined by dry weight on a Cahn microbalance (model 4700) and by phosphate analysis, matched to within 4%.

Synthesis of 1-palmitoyl-2-nervonoyl-phosphatidylcholine

The anhydride derivative of nervonic acid (24:$1^{\Delta 15(c)}$), prepared by the procedure of Selinger and Lapidot (1966), was reacted with 1-palmitoyl-2-hydroxy-phosphatidylcholine (lyso-PC) (Avanti Polar Lipids) in the presence of the catalyst, 4-pyrrolidino pyridine (molar ratio of lyso-PC/fatty acid anhydride/catalyst, 1:5:1) in chloroform under nitrogen at 30°C for 18 h to yield 1-palmitoyl-2-nervonoyl-*sn*-glycero-3-phosphocholine (PNPC) (Mason et al., 1981). The catalyst was removed by acid extraction using $CHCl_3/CH_3OH$/0.1 N HCl (6:3:2.2), and the lower phase was collected and dried. This mixture was then purified by flash column chromatography (230–400 mesh silica gel) using a step gradient consisting of $CHCl_3/CH_3OH$ (85:15) and $CHCl_3/CH_3OH/H_2O$ (65:35:8). The pure product, PNPC, was recrystallized and freed of silica gel as described above for GalCer. The final stock concentration of PNPC, determined by dry weight on a Cahn microbalance (model 4700) and by phosphate analysis, matched to within 4%.

Analysis of lipid purity and fatty acyl composition

Lipid purity was analyzed by TLC and was judged to be >99% using the solvent systems described by Ali et al. (1991) and Smaby et al. (1994). The acyl homogeneity of the synthesized lipids was determined by capillary gas-liquid chromatography after release and esterification of the fatty acyl moieties. Quantitative release of the amide-linked acyl chains was achieved by hydrolyzing 0.5 to 1.5 mg of each lipid in 2 ml of acetonitrile/0.5 M HCl (9:1; v/v) as described by Aveldano and Horrocks (1983). The released free fatty acids were trans-esterified by reacting with methanolic-HCl reagent (Supelco, Inc., Bellefonte, PA) at 90°C for 1 h. After extracting the fatty acid methyl esters with hexane, analysis was achieved by gas-liquid chromatography (Hewlett-Packard 5840A) using a 0.25-μm capillary column (J and W Scientific, Folsom, CA) as described by Cleary et al. (1994). The analysis showed the acyl homogeneity of all our synthetic GalCer, SM, and PC derivatives to be >99%. The acyl composition of the NFA-GalCer (Sigma, St. Louis, MO) was 3.3% (18:0), 3.4% (22:0), 4.0% (23:0), 16.9% (24:0), 67.7% (24:$1^{\Delta 15(c)}$), and 4.7% (25:0).

Preparation of aqueous lipid dispersions

The synthesized lipids were stored in a solvent mixture of hexane/isopropanol/water (70:30:2.5) at −20°C. The proper volume of lipid stock solution was dispensed into a round-bottom screw-cap vial. After evaporating the solvent under a stream of nitrogen, the lipid was dried in vacuo for a minimum of 4 h and was then dispersed in the required amount of phosphate buffer so as to obtain a final lipid concentration in the range of 0.5 to 5 mM. The phosphate buffer consisted of 10 mM potassium phosphate (pH 6.6) containing 100 mM sodium chloride and 1.5 mM sodium azide. The water used in the buffer was purified by reverse osmosis, mixed-bed deionization, adsorption on activated charcoal, and filtration through a 0.2-μm polycarbonate membrane. After adding buffer to the dried lipid, the suspension was incubated at 90°C for 3 min in a water bath and then was vigorously vortexed and briefly bath sonicated. After this process was repeated two more times, the dispersion was subjected to three freeze-thaw cycles to obtain uniform transbilayer distributions of the buffer solutes (Mayer et al., 1985). Rapid freezing was achieved by immersing the lipid suspension for about 2 min in an isopropanol/dry-ice bath. After the first two thawings, the dispersion was incubated at 90°C for 3 min and vortexed. After the final thawing, the dispersion was equilibrated to room temperature. This procedure did not cause any chemical breakdown of the lipid as revealed by TLC.

Electron microscopy

The preparation of the freeze-fracture replicas was essentially the same as we reported previously (Brown and Hyland, 1992; Brown et al., 1995). Briefly, small drops (~3 μl) of the lipid dispersion were placed on gold alloy planchets held at temperatures that ensured that the lipid was gel phase and then were flash frozen by plunging into liquid propane cooled by liquid nitrogen. Liquid propane was used for cryofixation because of its higher cooling rate (19,100°C/s) compared to Freon 22 (9,000°C/s), so that

slow-freezing artifacts could be avoided (Sternberg, 1992). No cryoprotectants such as glycerol were mixed with samples before cryofixation because of the structural changes known to be induced in GalCer samples by glycerol (see Brown et al., 1995, and references therein). The frozen samples were fractured and replicated at −120°C in a Balzers BAF-300 freeze-fracture apparatus equipped with a platinum/carbon shadowing gun (at 45° angle) and a carbon-evaporator. The replicas were cleaned in chloroform/methanol (2:1) and examined in a JEOL 100-S transmission EM.

Negatively stained samples were prepared by a procedure similar to that used by Archibald and Mann (1994) along with controls recommended by Forte and Nordhausen (1986). A small aliquot (5 μl) of the dispersion was placed on carbon-coated, 200-mesh copper grids, and the excess was carefully wicked away by touching a piece of filter paper to the edges of the grid. Staining was achieved by placing 5 μl of 2% uranyl acetate on the sample-coated grid and wicking away the excess stain by filter paper. To avoid drying and staining artifacts, variations also were employed in which equal volumes of uranyl acetate solution and the lipid dispersion (50 μl each) were mixed together and then applied to the carbon-coated grids as described above. Both methods of staining showed identical results. Several control grids (e.g., "staining" of buffer alone) also were examined to avoid artifacts and to confirm the structure of the lipid dispersion.

Differential scanning calorimetry

All thermotropic scans were obtained using a MC-2 microcalorimeter (Microcal Inc., Amherst, MA), which was equipped with the DT-2801 I/O data acquisition utility board for automated, computerized data collection. The lipid dispersions were degassed and then equilibrated in the calorimeter at 4°C under nitrogen for a minimum of 2 h before and between the scans. Data obtained in this manner were found to be no different than data obtained following 12- to 16-h incubations at 4°C. The microcalorimeter was calibrated using three different phospholipids of established thermotropic data (T_m ranging from 23°C to 72°C) as recommended by Schwarz (1991). Thermotropic data were analyzed using the Origin software package (Microcal Inc., Amherst, MA). The thermodynamic parameters reported here were obtained at a heating scan rate of 30°C/h. We found the thermotropic behavior of our GalCer samples to be highly reproducible only after the third heating scan. A similar observation was reported for the differential scanning calorimetry behavior of asymmetric chain length PCs (Lin and Huang, 1988). Hence, the thermograms shown in Fig. 5 were either the fourth or fifth scans.

RESULTS

Although high levels of nonaqueous solvents like ethylene glycol are known to promote formation of bilayer cylinders and tubules in naturally occurring GalCer (see Introduction), our recent experiments with NFA-GalCer/PC mixtures (Brown et al., 1995) as well as a few earlier studies involving GalCer (Yunis and Lee, 1970; Curatolo and Neuringer, 1986; Archibald and Yager, 1992) have indicated that cylindrical mesomorphic structures can also form under aqueous conditions. These observations raised the possibility that, under aqueous conditions, certain molecular species found in naturally occurring GalCer might phase separate and, as a result, could then self-assemble into bilayer cylinders that are either cochleate or tubular in nature.

To test this idea, we investigated the mesomorphic structure of *N*-lignoceroyl (24:0) GalSph and *N*-nervonoyl (24:$1^{\Delta 15(c)}$) GalSph, the two predominant species that make up NFA-GalCer (Johnson and Brown, 1992, and references therein). In the case of *N*-24:0 GalSph, which reportedly forms extraordinarily stable, interdigitated bilayers (Reed and Shipley, 1987), our freeze-fracture micrographs showed scattered, undulating, ribbon-like structures dominating the two-dimensional fracture planes (Fig. 2 *A*). The ribbon-like structures occasionally appeared to be twisted. The ribbon-like nature of the *N*-24:0 GalSph often resulted in separations along the ice-lipid juncture after the underlying lipid was dissolved away with chloroform-methanol.

The ribbon-like structures were more readily apparent in negative stain micrographs because of the sample layering achieved during negative stain preparation (Fig. 2, *B* and *C*). In this case, the ribbon-like structures appeared to be either extended or helically twisted. The long axial dimensions typically ranged from 2,000 to 10,000 nm, and the widths ranged from 100 to 250 nm. In general, it appeared that the tendency of the *N*-24:0 GalSph to appear helically twisted was accentuated under negative stain conditions. As detailed in Materials and Methods, rigorous control experiments revealed none of these high-axial structures in buffer preparations alone. The same appearance persisted regardless of whether the lipid dispersions were co-mixed with uranyl acetate before application to the carbon-coated EM grid or the lipid dispersions were dried on the EM grid before application of the uranyl acetate stain.

In contrast, N-24:$1^{\Delta 15(c)}$ GalSph aqueous dispersions revealed little evidence of the undulating ribbon-like structures that dominated the freeze fracture micrographs of N-24:0 GalSph. In fact, the freeze-fracture images of N-24:$1^{\Delta 15(c)}$ GalSph were dominated by tube-like structures, i.e., "nanotubes," that tended to aggregate into more or less self-aligned, long axial bundles (Fig. 3, *A* and *B*). The length of these tubular structures appeared to vary between 250 and 400 nm, with diameters of 25 to 30 nm. The diameter of the "nanotubes" provided indirect evidence that they were tubular and of single bilayer thickness. Previous studies of single bilayer vesicles have revealed that curvature-induced packing constraints restrict the lower-limit diameter to the range of 22 to 25 nm (Mason and Huang, 1978). Direct cross-sectional evidence verifying the single-walled nature of the "nanotubes" was difficult to obtain. Depending on tubule orientation relative to the freeze-fracture EM shadowing angle, tubules appeared as either hollow or filled, but never cochleate. The high-magnification micrographs (Fig. 3 *B*) of the "nanotubes" also revealed paired lines positioned along the edge and running the length of the tubules within the bundles. We suspect that these lines indicate either that small amounts of ice remain wedged between adjacent tubules after fracturing or that the platinum/carbon coating has a slight tendency to accumulate in the wedges between adjacent tubules. "Nanotubes" also dominated the negative stain images of *N*-24:$1^{\Delta 15(c)}$ GalSph (Fig. 3 *C*). However, because of the sample layering achieved in negative stain preparations, larger cylindrical structures also were visualized occasionally. The length of the larger tubular microstructures varied considerably (range, 5,000–10,000 nm),

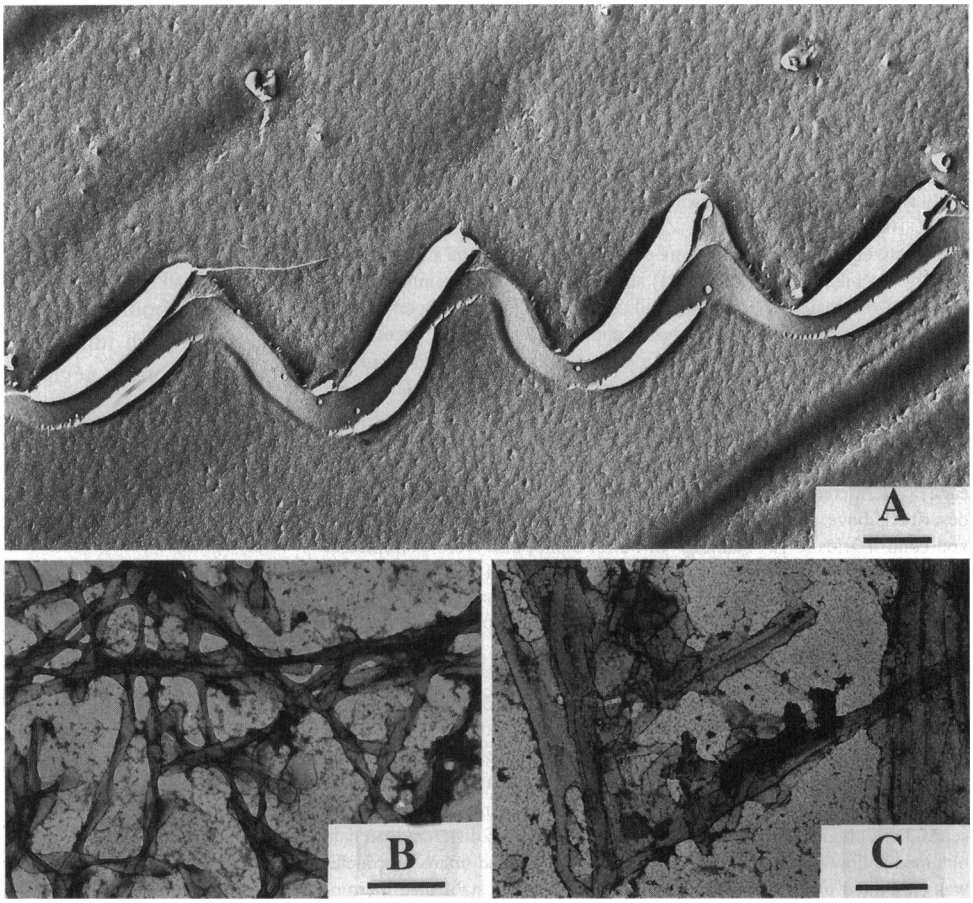

FIGURE 2 Morphology of *N*-lignoceroyl galactosylsphingosine (24:0 GalCer) aqueous dispersions. (*A*) Freeze fracture electron micrograph showing the undulating, ribbon-like structure typically observed in replicas. Samples were cryofixed from room temperature (≈22°C) by plunging into liquid propane after preparing as described in Materials and Methods. The bar in the lower right corner represents 500 nm. (*B*) Negative stain electron micrograph showing the helical twisting often observed in the ribbon-like structures. The bar represents 300 nm. (*C*) Negative stain electron micrograph showing non-twisted ribbon-like structures. The bar represents 400 nm. Samples were negatively stained from room temperature (≈22°C) after preparing as described in Materials and Methods.

but the diameter was relatively constant at 100 (±5) nm (Fig. 3 *C*).

We also examined the morphology of hydrated NFA-GalCer, which has a heterogeneous acyl composition dominated by nervonate (24:1$^{\Delta 15(c)}$) and by lignocerate (24:0) (see Materials and Methods). Freeze-fracture micrographs revealed that hydrated NFA-GalCer dispersions consisted mostly (90%) of scattered, rod-like, cylindrical structures (Fig. 4 *A*, arrows) along with occasional clusters of multilamellar liposomes (Fig. 4 *B*). The surfaces of the clustered liposomes were covered with a distinctive, jumbled, ridge-like pattern. Negative stain micrographs of NFA-GalCer, also showed the lipid assemblies to be mostly rod-like in appearance along with occasional interspersed multilamellar liposomes (Fig. 4 *C*). The dimensions of the long axial rod-like structures were 500 to 5,000 nm in length and 40 to 100 nm in width.

To confirm that the N-24:0 GalSph, N-24:1$^{\Delta 15(c)}$ GalSph, and NFA-GalCer dispersions were in similar phase states before ultra-rapid cryofixation or negative staining from room temperature, we investigated the thermotropic behavior of these GalCers by differential scanning calorimetry (DSC). To duplicate the conditions under which the EM studies were performed, all samples were freeze-thaw cycled (see Materials and Methods) before the first scan. Heating scans of N-24:1$^{\Delta 15(c)}$ GalSph dispersions (Fig. 5, trace 2) revealed two endothermic transitions, one centered at 59.3°C (ΔH = 7.0 kcal/mol) and another centered at 64.5°C (ΔH = 2.2 kcal/mol). Not surprisingly, the main thermal transition of N-24:0 GalSph occurred at much higher temperature. A sharp, large enthalpy transition was observed at 84.1°C and was followed by a smaller enthalpy transition at 85.7°C (Fig. 5, trace 1). The total enthalpy of the two transitions was 14.21 kcal/mol. This result was in general agreement with earlier DSC data published for N-24:0 GalSph (Reed and Shipley, 1987; Gardam and Silvius, 1989). Hence, it was clear that introducing a *cis* double bond at carbon 15 of the acyl chain had a major effect on the thermotropic behavior of N-24:0 GalSph. In fact, the effect was even greater than that reported for cerebroside sulfate with regard to the transition temperature "lowering effect" and the relative decline in enthalpy (Boggs et al., 1988a).

Surprisingly, we found that N-24:0 GalSph's thermotropic behavior differed significantly from that of a commercial N-24:0 dihydroGalSph. This latter sample showed two endothermic transitions, one centered at 71.0°C (ΔH = 12.7 kcal/mol) and the second centered at 77.3°C (ΔH = 6.6 kcal/mol) (data not shown). However, when analyzed by capillary GC, the N-24:0 dihydroGalSph was found to have acyl chains other than 24:0 (93.5%). Acyl chains of 22:0 and 18:1 accounted for 3.4% and 1.2%, respectively, and 1.8% were miscellaneous acyl chains. For this reason,

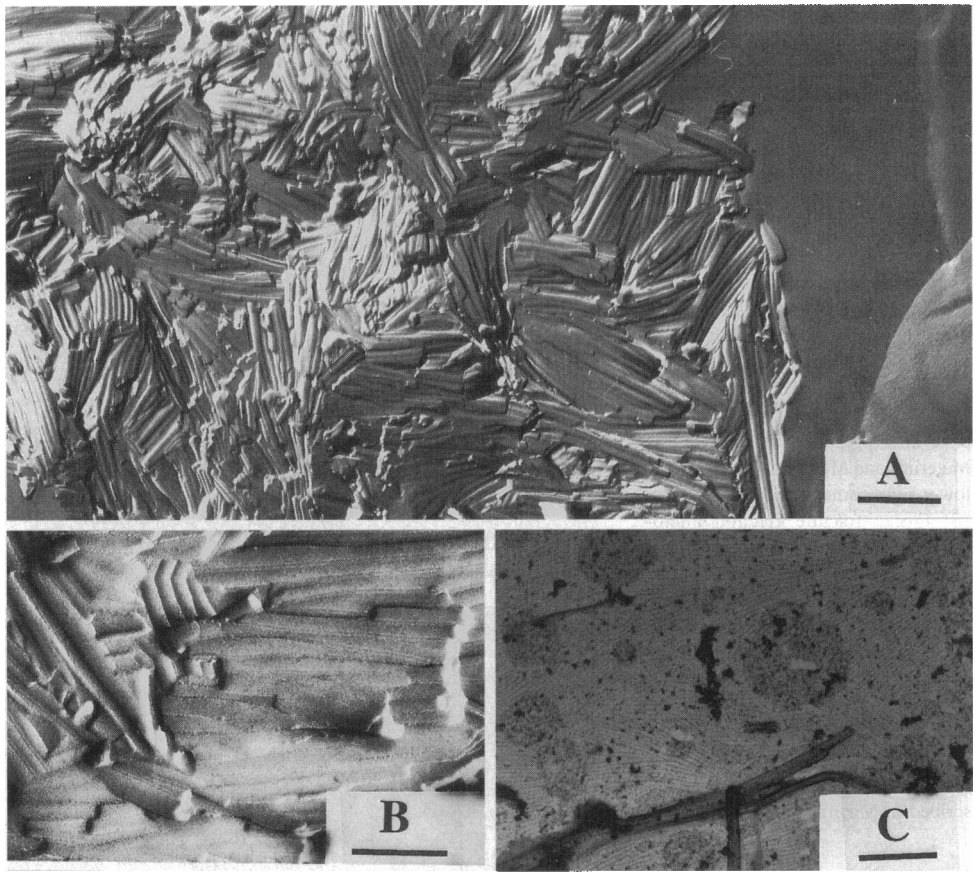

FIGURE 3 Morphology of *N*-nervonoyl galactosylsphingosine (24:1 GalCer) aqueous dispersions. (*A*) Freeze fracture electron micrograph showing the bundles of "nanotubes" typically observed in replicas. Samples were cryofixed from room temperature (≈22°C) by plunging into liquid propane after preparing as described in Materials and Methods. The bar in the lower right corner represents 250 nm. (*B*) Freeze fracture electron micrograph showing higher magnification view of the "nanotubes." The bar represents 150 nm. (*C*) Negative stain electron micrograph showing bundles of "nanotubes" typically observed along with a few larger cylinders. The bar represents 350 nm. Samples were negatively stained from room temperature (≈22°C) after preparing as described in Materials and Methods.

further investigations will be needed to resolve what effect the dihydro sphingoid base has on the DSC behavior of homogeneously acylated GalCer species.

For NFA-GalCer, we observed one endothermic transition centered at 69.5°C (ΔH = 7.7 kcal/mol) and another centered at 75.0°C (ΔH = 5.5) (Fig. 5, trace 3). Capillary GC analysis of this NFA-GalCer sample revealed its acyl composition to be 24:1$^{\Delta 15(c)}$ (68%), 24:0 (17%), 25:0 (5%), 23:0 (4%), 22:0 (3%), and 18:0 (2%). Curatolo and Jungalwala (1985) reported that a NFA-GalCer subfraction with an acyl composition consisting of 24:1$^{\Delta 15(c)}$ (73%), 22:0 (23%), and 25:0 (3.4%) displayed a major endothermic transition at 70°C and a smaller transition at 75°C. Hence, our DSC studies of NFA-GalCer (as well as N-24:0 GalSph and N-24:1$^{\Delta 15(c)}$ GalSph) confirmed that room temperature equilibration resulted in comparable lipid phase states for the EM analyses.

Role of lipid interface/headgroup structure in tubule/cylinder formation

We found the morphological results obtained with N-24:0 GalSph (24:0 GalCer), N-24:1$^{\Delta 15(c)}$ GalSph (24:1 GalCer), and NFA-GalCer dispersions to be quite interesting because our earlier studies showed hydrated dispersions of bovine brain GalCer, which has both nonhydroxy and 2-hydroxy acyl chains, to be mostly multilamellar liposomal-like assemblies (Brown et al., 1995). Other researchers have made similar observations (Maggio et al., 1988). This result pointed to the HFA-GalCer as necessary for liposome formation and suggested that changes to the polar headgroup and/or interfacial region were essential in determining whether GalCer forms cylindrical tubes or liposomes under aqueous conditions. This idea seemed plausible because the location of 2-hydroxyl groups in HFA-GalCer is known to be at the interfacial region separating the nonpolar hydrocarbons from the polar headgroup (Sundell and Pascher, 1977). Furthermore, the presence of the 2-hydroxyl groups increases the hydration level of the interfacial region and is thought to play a role in preventing dehydration events that can lead to metastability in naturally occurring GalCer (Curatolo, 1982).

To determine whether headgroup structure plays a key role in modulation of bilayer tubule formation, we investigated the mesomorphic phase structure of aqueous dispersions of sphingomyelin (SM) containing nervonoyl acyl chains (*N*-24:1$^{\Delta 15(c)}$ sphingosylphosphorylcholine). Because the sphingoid base chain was similar to that found in GalCer, the structural differences were directed to the headgroup region, where galactose was replaced by the zwitterion phosphocholine. However, to be sure that the EM studies of 24:1 SM were comparable to 24:1 GalCer with respect to phase state, we investigated the thermotropic behavior of 24:1 SM aqueous dispersions by DSC. When

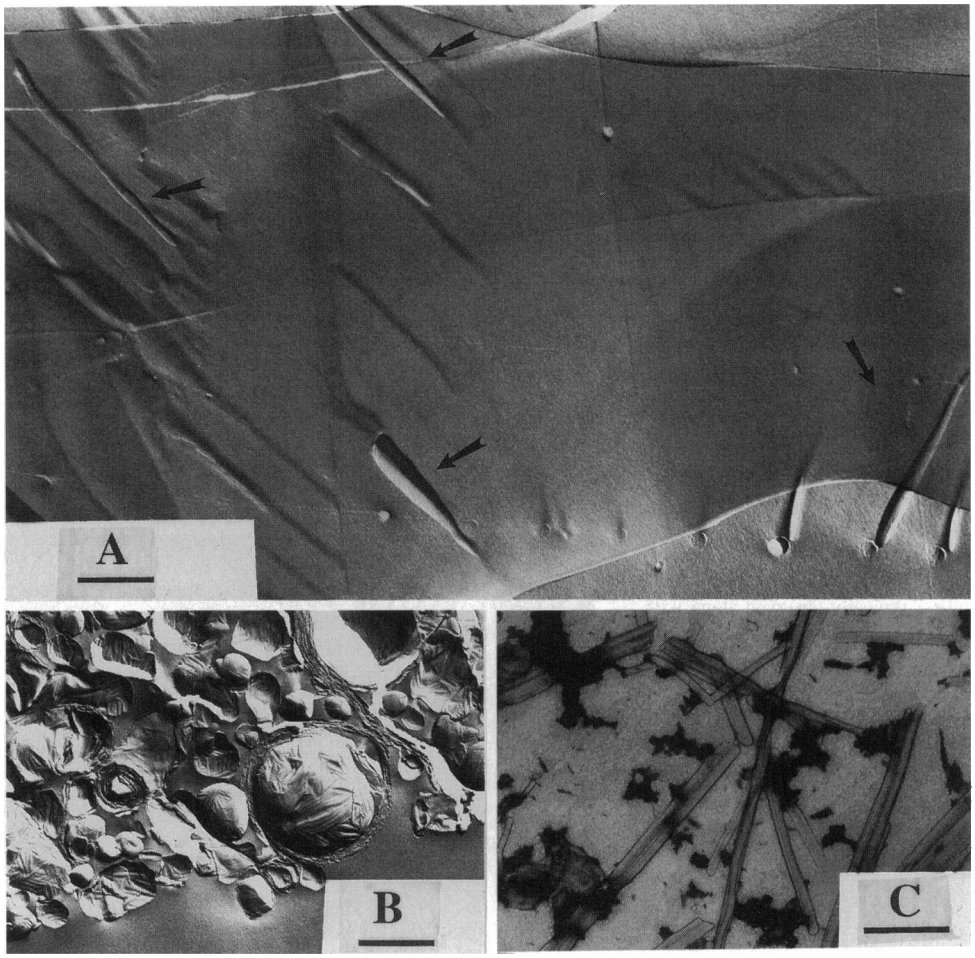

FIGURE 4 Morphology of bovine brain GalCer subfraction containing naturally occurring mixture of nonhydroxy acyl chains (NFA-GalCer). (*A*) Freeze fracture electron micrograph showing the cylindrical structures typically observed in replicas (arrows indicate areas with cylindrical structures). Samples were cryofixed from room temperature (≈22°C) by plunging into liquid propane after preparing as described in Materials and Methods. The bar in the lower right corner represents 500 nm. (*B*) Freeze fracture electron micrograph showing a cluster of liposomal-like structures that are occasionally observed. The bar represents 500 nm. (*C*) Negative stain electron micrograph showing the cylinders typically observed along with a few liposomal-like structures (*lower left*). The bar represents 500 nm. Samples were negatively stained from room temperature (≈22°C) after preparing as described in Materials and Methods.

prepared in the same manner as 24:1 GalCer, 24:1 SM dispersions showed a single, broad, low-enthalpy transition during heating scans (T_m = 22.3°C; ΔH = 1.4 kcal/mol) (Fig. 5, trace 4). Hence, for freeze-fracture EM analyses, we equilibrated our aqueous dispersions of 24:1 SM at 10°C before cryofixation.

Fig. 6 *A* shows a typical freeze-fracture micrograph, dominated by multilamellar liposomes that exhibited striking multifaceted, polyhedral surfaces and that occasionally displayed zig-zagging, ridge-like structures. Virtually no traces of cylindrical or tubular structures were evident. Negative-stain micrographs in which both the 24:1 SM and uranyl acetate stain were maintained at 10°C during specimen preparation also showed only multilamellar liposomes that often were clumped together (Fig. 6 *B*). However, many of the liposomes (30–40%) showed evidence of being shaped like biconcave discs and "dumbbells" rather than like spheres. Sphingomyelin's propensity to form distended blebs in conduction with fission events has been noted previously (Sackmann, 1994).

To determine whether the unusual surface structure and interesting morphological shapes of 24:1 SM were related to its sphingoid nature, we also investigated the glycerol-based analog, 1-palmitoyl-2-nervonoyl PC (PNPC). As we have pointed out in other recent studies, SM and PC are quite

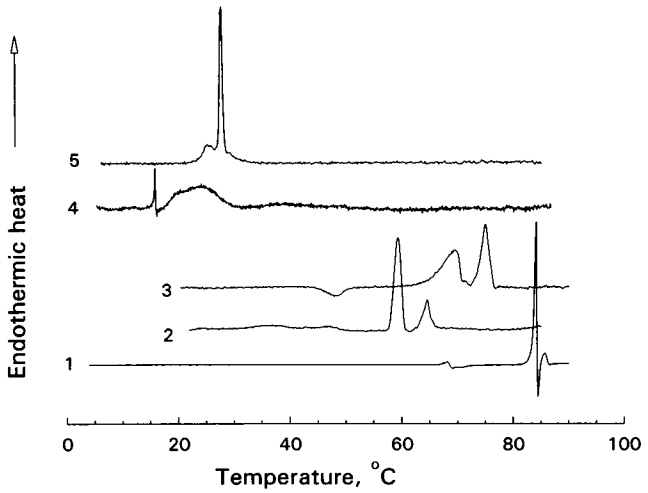

FIGURE 5 Differential scanning calorimetric thermal behavior of aqueous lipid dispersions. All traces are heating scans run at a rate of 30°C/h. In each case the thermogram is either the fourth or fifth scan of a given sample because we found the thermotropic behavior of our GalCer samples to be highly reproducible only after the third heating scan. Other experimental details are described in Materials and Methods. Trace 1, *N*-lignoceroyl galactosylsphingosine (24:0 GalCer). Trace 2, *N*-nervonoyl galactosylsphingosine (24:1 GalCer). Trace 3, NFA-GalCer. Trace 4, *N*-nervonoyl sphingosylphosphorylcholine (24:1 SM). Trace 5, 1-palmitoyl-2-nervonoyl phosphatidylcholine (PNPC).

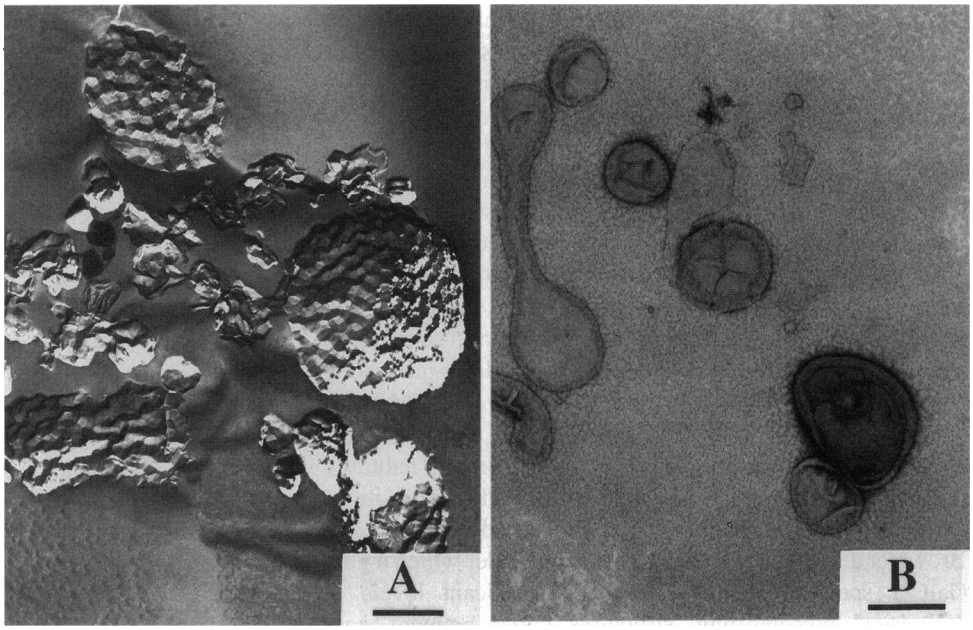

FIGURE 6 Morphology of *N*-nervonoyl sphingosylphosphorylcholine (24:1 SM) aqueous dispersions. (*A*) Freeze fracture electron micrograph showing the liposomes with multifaceted, polyhedral surface texture typically observed in replicas. Samples were cryofixed from ≈10°C by plunging into liquid propane after preparing as described in Materials and Methods. The bar in the lower right corner represents 500 nm. (*B*) Negative stain electron micrograph showing liposomes typically observed, including discoid and dumbbell shaped self-assemblies. The bar represents 400 nm. Samples were negatively stained from ≈10°C after preparing as described in Materials and Methods.

similar from a configurational and structural standpoint when the *sn*-1 chain of PC is palmitate and the *sn*-2 chain matches SM's acyl chain (Smaby et al., 1994). For this reason, we synthesized and purified PNPC (see Materials and Methods). Before investigating the morphology of PNPC dispersions, we characterized its thermotropic behavior by DSC. In this way, we could verify PNPC's phase state during the morphological studies.

Heating scans revealed that PNPC exhibits a single endothermic transition centered at 27.7°C (ΔH = 8.9 kcal/mol) that is preceded by a small "pretransition" (Fig. 5, trace 5). The calorimetric data of Wang et al. (1995) also support these findings. As with 24:1 SM, we equilibrated our aqueous dispersions of PNPC at 10°C before cryofixation for EM analysis. However, in contrast to the appearance of 24:1 SM (Fig. 6 *A*), PNPC dispersions consisted of multilamellar liposomes with relatively smooth surface features but variable and somewhat discontinuous fracture planes (Fig. 7 *A*). Virtually no traces of cylindrical or tubular structures were evident. Negative-stain EM analyses also showed only multilamellar liposomes that were sometimes clumped, with no evidence of the cylindrical or tubular structures (Fig. 7 *B*).

DISCUSSION

Although lipid tubules and cochleate bilayer cylinders had been observed previously in aqueous lipid dispersions con-

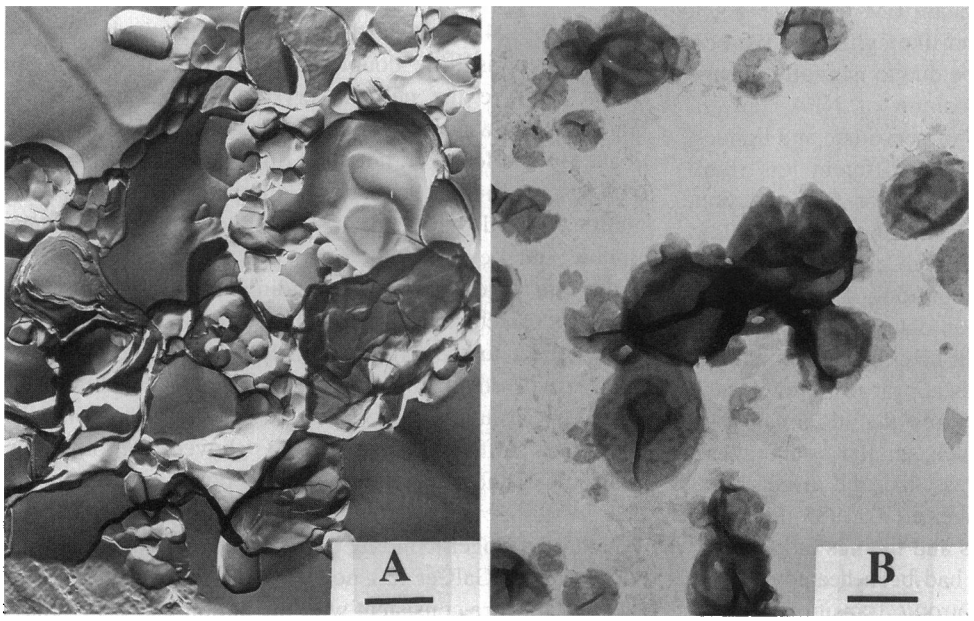

FIGURE 7 Morphology of 1-palmitoyl-2-nervonoyl phosphatidylcholine (PNPC) aqueous dispersions. (*A*) Freeze fracture electron micrograph showing liposomes with smooth surface textures typically observed in replicas. Samples were cryofixed from ≈10°C by plunging into liquid propane after preparing as described in Materials and Methods. The bar in the lower right corner represents 500 nm. (*B*) Negative stain electron micrograph showing liposomes typically observed, including occasional discoid shaped self-assemblies. The bar represents 500 nm. Samples were negatively stained from ≈10°C after preparing as described in Materials and Methods.

taining naturally occurring GalCer, the molecular species promoting tubular mesophase formation was not clear. Our results indicate that, under aqueous conditions, 24:1 GalCer, the predominant monounsaturated, nonhydroxy acyl species of bovine brain GalCer, forms cylindrical mesomorphic self-assemblies, including lipid bilayer tubules of more or less uniform length and diameter. In contrast, 24:0 GalCer, the major saturated, nonhydroxy acyl species of bovine brain GalCer, displays no tendency to form such tubules. Instead, 24:0 GalCer prefers to form large, variable-length ribbon-like structures that appear wavy and, sometimes, helically twisted. These findings are particularly interesting because, until now, the formation of GalCer bilayer tubules and cylinders under aqueous conditions was thought to be a somewhat rare event based on investigations of naturally occurring GalCer with heterogeneous acyl compositions (e.g., Yunis and Lee, 1970; Archibald and Yager, 1992; Brown et al., 1995). The only conditions under which a pure GalCer species reportedly formed significant levels of cylindrical mesomorphic structures under aqueous conditions was that of 16:0 GalCer, which is at best only a trace component of bovine brain GalCer (Curatolo and Neuringer, 1986). In fact, solvation conditions requiring a high concentrations of ethylene glycol were thought to be necessary to achieve significant cylinder and/or tubule formation among naturally occurring GalCer species (Yager et al., 1992; Archibald and Mann, 1994). In this respect, ethylene glycol was judged to be unique among many hydroxyl-containing solvents, including various mono-ols, diols, and triols of varying hydrophobicity in varying proportions with water.

Interestingly, our findings regarding the rod-like morphology of NFA-GalCer agree with an earlier report by Curatolo and Neuringer (1986) but appear to be at odds with the findings of Archibald and Yager (1992), who reported multilamellar aggregates of liposomes to be the predominant structural assembly in NFA-GalCer aqueous dispersions, even though their negative-stain EM image (Fig. 2) included substantial amounts of rod-like cylinders. We believe this discrepancy is likely to be due to naturally occurring variation in the acyl composition of NFA-GalCer, because we have found the amount of nervonate and lignocerate to vary by as much as 30% in different lots from commercial suppliers. Possible reasons for this variation have been discussed previously (Johnson and Brown, 1992).

Our morphological results with GalCer are in general agreement with previous reports regarding the phase state under which tubular bilayers form in diacetylenic PC aqueous dispersions. However, it should be emphasized that the tubules formed by diacetylenic PCs appear to more closely resemble the large rod-like structures that dominate our NFA-Gal dispersions than the much smaller "nanotubes" formed by 24:1 GalCer. Nonetheless, like the diacetylenic PCs (Yager and Schoen, 1984; Yager et al., 1985; Rudolph and Burke 1987), bilayer cylinders and tubules did form in NFA-GalCer or 24:1 GalCer that had been heated to temperatures above their main thermotropic transitions before cooling below T_m. In our case, freeze-thaw thermal cycling also was employed (see Materials and Methods) to achieve uniform transbilayer distribution of buffer salts (Mayer et al., 1985) before the final thawing and subsequent slow equilibration to temperatures below T_m. In this respect, the results that we obtained with NFA-GalCer and 24:1 GalCer agree with a recent report by Thomas et al. (1995), who proposed that formation of diacetylenic PC bilayer cylinders in ethanolic solutions is driven by a first-order freezing transition involving in-plane two-dimensional ordering. For diacetylenic PCs, the basic tubule structure is believed to be established during the two-dimensional freezing process, with the ordered state growing from narrow bilayer ribbons, which spontaneously curl in response to the system chirality. This idea is quite similar to that of Schnur et al. (1994), who proposed that large vesicles or multilamellar aggregates of diacetylenic PC, upon cooling below T_m, develop bilayer stripes due to chiral molecular orientation. The stripes are separated by sharp domain walls. The break-up of vesicles or lipid aggregates along these domain walls leads to ribbon formation. The key point with regard to chiral packing is that long chiral molecules do not pack parallel to but rather at a non-zero twist angle with respect to their nearest neighbors (Singh et al., 1988; Yager et al., 1992; Schnur et al., 1994). When the chiral molecules are constrained to a bilayer phase in which the molecules tilt with respect to the local layer normal, the favored twist from neighbor to neighbor leads the whole phase to twist into a helical ribbon that may either be stable or may fuse into a cylinder to reduce its edge energy. Yager et al. (1992) also have pointed out the possibility that, within the plane of a monolayer, the strong linear associations necessary to stabilize tubule and helix formation in GalCers could be optimized by hydrogen bonding interactions.

The above model raises interesting possibilities regarding tubule formation in aqueous dispersions of 24:1 GalCer as well as the cylinder and ribbon formation in the NFA-GalCer and 24:0 GalCer dispersions, respectively. For instance, there is little doubt that intermolecular hydrogen bonds stabilize the gel and crystalline phases of NFA-GalCer (Bunow and Levin, 1980) and of 16:0 GalCer (Pink et al., 1988). However, not all hydrogen bonds are the same with respect to their impact on GalCer's headgroup conformation. Based on Raman spectroscopic measurements, Bunow and Levin (1980) point out that strong hydrogen bonds are involved in the bending of crystalline HFA-GalCer's galactose headgroup into a "shovel" conformation with respect to the hydrocarbon long axis. The hydrogen bonds involved in this scheme are stronger than those of NFA-GalCer and, upon conversion to a hydrated gel state, undergo a shift that may relax the "shovel" conformation. Elements of these different hydrogen bonding schemes appear to survive in the natural bovine brain GalCer mixture. Whether hydrogen bonding persists in unsaturated GalCers such as 24:1 GalCer has not yet been determined. All of these factors are consistent with the notion that the strength

and directionality of the hydrogen bonds may be key factors in bilayer tubule/-cylinder formation.

Another parameter that may play a role in whether tubules form is the presence or absence of transbilayer hydrocarbon interdigitation among different GalCer molecular species. Despite the large hydrocarbon chain length asymmetry that exists in GalCer molecular species such as 24:1 GalCer, the presence of the *cis* double bond may prevent hydrocarbon interdigitation, such as that which occurs in gel phase 24:0 GalCer (Reed and Shipley, 1987). Indeed, we found that 24:0 GalCer formed ribbon-like structures, but no bilayer tubules. Based on spin-label mobility measurements, Boggs et al. (1988b) have suggested that the nervonoyl species of cerebroside sulfate is not interdigitated at all in the metastable gel phase. A similar condition may contribute to the curvature-stabilizing interactions among 24:1 GalCer molecules thought to be necessary to maintain stable cylindrical shape (Yager et al., 1992). Evidence that interdigitation is a not necessary condition for bilayer tubule formation also comes from recent x-ray diffraction measurements of diacetylenic PC by Thomas et al. (1995), who reported a complete lack of interdigitation in the crystalline tubule phase, even though interdigitation was observed in the chain-melted multilamellar vesicle phase. Nevertheless, the fact that the phosphocholine headgroup supports cylinder formation when attached to the diacetylenic glycerol moiety but not to the palmitoyl-nervonoyl glycerol moiety or the *N*-24:1$^{\Delta 15(c)}$ sphingosine moiety further emphasizes the multiplicity of parameters that are likely to be involved.

Understanding the formation of bilayer cylinders and tubules is likely to have important implications in the biomedical and biomaterials fields. For instance, helical and tubular microstructures form as cholesterol crystallizes from bile, a process of clinical relevance during gallstone formation (Konikoff et al., 1992). The helical ribbons are believed to be metastable intermediates that occur in response to the cholesterol molecules organizing into tilted chiral phases during the crystallization process (Chung et al., 1993). Such insights may provide new ways to design inhibitors of cholesterol gallstone formation. Also, by studying how systematic structural alterations of biological amphiphiles (e.g., GalCer) affect resulting mesomorphic phase structure, it may be possible to engineer molecules to produce a desired self-assembly of specified dimensions (e.g., hollow cylinders). Such structures would be useful as templates for certain types of metallization processes in which stable and durable nanotubes are desired (Schnur, 1993; Archibald and Mann, 1993).

We thank Fred Phillips and Margot Cleary for their help with the capillary GC analyses and Kristi Hyland for synthesizing and purifying the 24:0 GalCer. This investigation was supported by U.S. Public Health Service grant GM45928 and the Hormel Foundation.

REFERENCES

Ahmed, T. Y., J. T. Sparrow, and J. D. Morrisett. 1985. Fluorine-, pyrene-, and nitroxide-labeled sphingomyelin: semi-synthesis and thermotropic properties. *J. Lipid Res.* 26:1160–1165.

Ali, S., H. L. Brockman, and R. E. Brown. 1991. Structural determinants of miscibility in surface films of galactosylceramide and phosphatidylcholine: effect of unsaturation in the galactosylceramides acyl chain. *Biochemistry.* 30:11198–11205.

Ali, S., J. M. Smaby, and R. E. Brown. 1993. Acyl structure regulates galactosylceramide's interfacial interactions. *Biochemistry.* 32: 11696–11703.

Ali, S., J. M. Smaby, and R. E. Brown. 1994. Galactosylceramides with homogeneous acyl chains: the effect of acyl structure on intermolecular interactions occurring at the argon/buffered saline interface. *Thin Solid Films.* 244:860–864.

Archibald, D. D., and S. Mann. 1993. Template mineralization of self-assembled anisotropic lipid microstructures. *Nature.* 364:430–433.

Archibald, D. D., and S. Mann. 1994. Self-assembled microstructures from 1,2-ethanediol suspensions of pure and binary mixtures of neutral and acidic biological galactosylceramides. *Chem. Phys. Lipids.* 69:51–64.

Archibald, D. D., and P. Yager. 1992. Microstructural polymorphism in bovine brain galactocerebroside and its two major subfractions. *Biochemistry.* 31:9045–9055.

Aveldano, M. I., and L. A. Horrocks. 1983. Quantitative release of fatty acids from lipids by a simple hydrolysis procedure. *J. Lipid Res.* 24: 1101–1105.

Boggs, J. M., K. M. Koshy, and G. Rangaraj. 1988a. Influence of structural modifications on the phase behavior of semi-synthetic cerebroside sulfate. *Biochim. Biophys. Acta.* 938:361–372.

Boggs, J. M., K. M. Koshy, and G. Rangaraj. 1988b. Interdigitated lipid bilayers of long acyl chain species of cerebroside sulfate. A fatty acid spin label study. *Biochim. Biophys. Acta.* 938:373–385.

Brown, R. E., W. H. Anderson, and V. S. Kulkarni. 1995. Macro-ripple phase formation in bilayers composed of galactosylceramide and phosphatidylcholine. *Biophys. J.* 68:1396–1405.

Brown, R. E., and K. J. Hyland. 1992. Spontaneous transfer of ganglioside GM1 from its micelles to lipid vesicles of differing size. *Biochemistry.* 31:10602–10609.

Bunow, M. R. 1979. Two gel states of cerebrosides: calorimetric and Raman spectroscopic evidence. *Biochim. Biophys. Acta.* 574:542–546.

Bunow, M. R., and I. W. Levin. 1980. Molecular conformations of cerebrosides in bilayers determined by Raman spectroscopy. *Biophys. J.* 32:1007–1021.

Chung, D. S., G. B. Benedek, F. M. Konikoff, and J. M. Donovan. 1993. Elastic free energy of anisotropic helical ribbons as metastable intermediates in the crystallization of cholesterol. *Proc. Natl. Acad. Sci. USA.* 90:11341–11345.

Cleary, M. P., F. C. Phillips, and R. A. Morton. 1994. Liver, serum and adipose tissue fatty acid composition in suckling Zucker rats. *Lipids.* 29:753–758.

Cohen, R., Y. Barenholz, and A. Dagan. 1984. Preparation and characterization of well defined D-erythro sphingomyelins. *Chem. Phys. Lipids.* 35:371–384.

Curatolo, W. 1982. Thermal behavior of fractionated and unfractionated bovine brain cerebrosides. *Biochemistry.* 21:1761–1764.

Curatolo, W. 1987. The physical properties of glycolipids. *Biochim. Biophys. Acta.* 906:111–136.

Curatolo, W., and F. B. Jungalwala. 1985. Phase behavior of galactocerebrosides from bovine brain. *Biochemistry.* 24:6608–6613.

Curatolo, W., and L. J. Neuringer. 1986. The effects of cerebrosides on model membrane shape. *J. Biol. Chem.* 261:17177–17182.

Díaz, R. S., and J. Monreal. 1994. Unusual low proton permeability of liposomes prepared from the endogenous myelin lipids. *J. Neurochem.* 62:2022–2029.

Forte, T. M., and R. W. Nordhausen. 1986. Electron microscopy of negatively stained lipoproteins. *Methods Enzymol.* 128:442–457.

Gardam, M., and J. R. Silvius. 1989. Intermixing of dipalmitoylphosphatidylcholine with phospho- and sphingolipids bearing highly asymmetric hydrocarbon chains. *Biochim. Biophys. Acta.* 980:319–325.

Jackson, M., D. S. Johnston, and D. Chapman. 1988. Differential scanning calorimetric and Fourier transform infrared spectroscopic investigations of cerebroside polymorphism. *Biochim. Biophys. Acta.* 944:497–506.

Johnson, S. B., and R. E. Brown. 1992. Simplified derivatization for determining sphingolipid fatty acyl composition by gas chromatography-mass spectrometry. *J. Chromatogr.* 605:281–286.

Kates, M. 1986. Separation of lipid mixtures. *In* Laboratory Techniques in Biochemistry and Molecular Biology, Vol. 3. Techniques of Lipidology, Pt. 2. Isolation. Analysis and Identification of Lipids. R. H. Burdon and B. H. Van Knippenberg, editors. Elsevier, Amsterdam. 186–278.

Kodama, M., T. Miyata, and T. Yokoyama. 1993. Crystalline cylindrical structures of Na^+-bound dimyristoylphosphatidylglycerol as revealed by microcalorimetry and electron microscopy. *Biochim. Biophys. Acta.* 1168:243–248.

Konikoff, F. M., D. S. Chung, J. M. Donovan, D. M. Small, and M. C. Carey. 1992. Filamentous, helical, and tubular microstructures during cholesterol crystallization from bile. *J. Clin. Invest.* 90:1155–1160.

Koynova, R., and M. Caffrey. 1995. Phases and phase transitions of the sphingolipids. *Biochim. Biophys. Acta.* 1255:213–236.

Lapidot, Y., S. Rappoport, and Y. Wolman. 1967. Use of esters of N-hydroxysuccinimide in the synthesis of N-acylaminoacids. *J. Lipid Res.* 8:142–145.

Lee, D. C., I. R. Miller, and D. Chapman. 1986. An infrared spectroscopic study of metastable and stable forms of hydrated cerebroside bilayers. *Biochim. Biophys. Acta.* 859:266–270.

Lin, H., and C. Huang. 1988. Eutectic phase behavior of 1-stearoyl-2-capryl phosphatidylcholine and dimyristoylphosphatidylcholine mixtures. *Biochim. Biophys. Acta.* 946:178–184.

Lin, K. C., R. M. Weiss, and H. M. McConnell. 1982. Induction of helical liposomes by Ca^{++} mediated intermembrane binding. *Nature.* 296: 164–165.

Maggio, B. 1994. The surface behavior of glycosphingolipids in biomembranes: a new frontier in molecular ecology. *Prog. Biophys. Mol. Biol.* 62:55–117.

Maggio, B., J. Albert, and R. K. Yu. 1988. Thermodynamic-geometric correlations for the morphology of self-assembled structures of glycosphingolipids and their mixtures with dipalmitoylphosphatidylcholine. *Biochim. Biophys. Acta.* 945:145–160.

Mason, J. T., A. V. Broccoli, and C. Huang. 1981. A method for the synthesis of isomerically pure saturated mixed chain phosphatidylcholines. *Anal. Biochem.* 113:96–101.

Mason, J. T., and C. Huang. 1978. Hydrodynamic analysis of egg phosphatidylcholine vesicles. *Ann. NY Acad. Sci.* 308:29–49.

Mayer, L. D., M. J. Hope, P. R. Cullis, and A. S. Janoff. 1985. Solute distributions and trapping efficiencies observed in freeze-thawed multilamellar vesicles. *Biochim. Biophys. Acta.* 817:193–196.

Mishima, K., T. Ogihara, M. Tomita, and K. Satoh. 1992. Growth rate of myelin figures for phosphatidylcholine and phosphatidylethanolamine. *Chem. Phys. Lipids.* 62:87–91.

Naito, M., K. Takahashi, and H. Hojo. 1988. An ultrastructural and experimental study on the development of tubular structures in the lysosomes of Gaucher cells. *Lab. Invest.* 58:590–598.

Nakashima, N., S. Asakuma, and T. Kunitake. 1985. Optical microscopic study of helical superstructures of chiral bilayer membranes. *J. Am. Chem. Soc.* 107:509–510.

O'Brien, J. S., and E. L. Sampson. 1965. Lipid composition of the normal human brain: gray matter, white matter, and myelin. *J. Lipid Res.* 6:537–544.

Pascher, I., and S. Sundell. 1977. Molecular arrangements in sphingolipids: the crystal structure of cerebroside. *Chem. Phys. Lipids.* 20:175–191.

Pink, D. A., A. L. MacDonald, and B. Quinn. 1988. Anisotropic interactions in hydrated cerebrosides: a theoretical model of stable and metastable states and hydrogen-bond formation. *Chem. Phys. Lipids.* 47: 83–95.

Radin, N. S. 1974. Preparation of psychosines (1-O-hexosyl sphingosine) from cerebrosides. *Lipids.* 9:358–360.

Reed, R. A., and G. G. Shipley. 1987. Structure and metastability of N-lignocerylgalactosylsphingosine (cerebroside) bilayers. *Biochim. Biophys. Acta.* 896:153–164.

Reed, R. A., and G. G. Shipley. 1989. Effect of chain unsaturation on the structure and thermotropic properties of galactocerebrosides. *Biophys. J.* 55:281–292.

Rudolph, A. S., and T. G. Burke. 1987. A Fourier-transform infrared spectroscopic study of the polymorphic phase behavior of 1,2-bis(tricosa-10, 12-diynoyl)-*sn*-glycero-3-phosphocholine; a polymerizable lipid which forms novel microstructures. *Biochim. Biophys. Acta.* 902:349–359.

Rudolph, A. S., B. R. Ratna, and B. Kahn. 1991. Self-assembling phospholipid filaments. *Nature.* 352:52–55.

Ruocco, M. J., G. G. Shipley, and E. Oldfield. 1983. Galactocerebroside-phospholipid interactions in bilayer membranes. *Biophys. J.* 43:91–101.

Sackmann, E. 1994. Membrane bending energy concept of vesicle- and cell-shapes and shape-transitions. *FEBS Lett.* 346:3–16.

Schnur, J. M. 1993. Lipid tubules: a paradigm for molecularly engineered structures. *Science.* 262:1669–1676.

Schnur, J. M., R. Price, P. Schoen, P. Yager, J. M. Calvert, J. Georger, and A. Singh. 1987. Lipid-based tubule microstructures. *Thin Solid Films.* 152:181–206.

Schnur, J. M., B. R. Ratna, J. V. Selinger, A. Singh, G. Jyothi, and K. R. K. Easwaran. 1994. Diacetylenic lipid tubules: experimental evidence for a chiral molecular architecture. *Science.* 264:945–947.

Schoen, P. E., R. R. Price, J. M. Schnur, A. Gulik, and T. Gulikkrzywicki. 1993. Formation of lipid tubule microstructures - time-resolved freeze-fracture electron microscopy and X-ray characterization. *Chem. Phys. Lipids.* 65:179–191.

Schwarz, F. P. 1991. Biological thermodynamic data for the calibration of differential scanning calorimeters: dynamic temperature data on the gel to liquid crystal phase transition of dialkylphosphatidylcholine in water suspensions. *Thermochim. Acta.* 177:285–303.

Schwarzmann, G., and K. Sandhoff. 1987. Lysogangliosides: synthesis and use in preparing labeled gangliosides. *Methods Enzymol.* 138: 319–341.

Selinger, Z., and Y. Lapidot. 1966. Synthesis of fatty acid anhydrides by reaction with dicyclohexylcarbodiimide. *J. Lipid Res.* 7:174–175.

Singh, A., J. Georger, R. R. Price, T. Burke, P. E. Schoen, and P. Yager. 1988. Lateral phase separation based on chirality in a polymerizable lipid and its influence on formation of tubular microstructures. *Chem. Phys. Lipids.* 47:135–148.

Smaby, J. M., H. L. Brockman, and R. E. Brown. 1994. Cholesterol's interfacial interactions with sphingomyelins and phosphatidylcholines: hydrocarbon chain structure determines the magnitude of condensation. *Biochemistry.* 33:9135–9142.

Sternberg, B. 1992. Freeze-fracture electron microscopy of liposomes. *In* Liposome Technology, 2nd ed., Vol. 1. G. Gregoridadis, editor. CRC Press, Boca Raton, FL. 363–383.

Svennerholm, L., K. Boström, P. Fredman, B. Jungbjer, J.-E. Månsson, and B.-M. Rynmark. 1992. Membrane lipids of human peripheral nerve and spinal cord. *Biochim. Biophys. Acta.* 1128:1–7.

Thomas, B. N., C. R. Safinya, R. J. Plano, and N. A. Clark. 1995. Lipid tubule self-assembly: length dependence on cooling rate through a first-order phase transition. *Science.* 267:1635–1637.

Thompson, T. E., and T. W. Tillack. 1985. Organization of glycosphingolipids in bilayers and plasma membranes of mammalian cells. *Annu. Rev. Biophys. Biophys. Chem.* 14:361–386.

Wang, Z., H. Lin, S. Li, and C. Huang. 1995. Phase transition behavior and molecular structures of monounsaturated phosphatidylcholines. *J. Biol. Chem.* 270:2014–2023.

Yager, P., J. Chappell, and D. D. Archibald. 1992. When lipid bilayers won't form liposomes: tubules, helices, and cochleate cylinders. *In* Biomembrane Structure and Function—The State of the Art. B. P. Gaber and K. R. K. Easwaran, editors. Adenine Press, Schenectady, New York. 1–18.

Yager, P., and P. E. Schoen. 1984. Formation of tubules by a polymerizable surfactant. *Mol. Cryst. Liq. Cryst.* 106:371–381.

Yager, P., P. E. Schoen, C. Davies, R. Price,, and A. Singh. 1985. Structure of lipid tubules formed from a polymerizable lecithin. *Biophys. J.* 48:899–906.

Yunis, E. J., and R. E. Lee. 1970. Tubules of globoid leukodystrophy: a right-handed helix. *Science.* 169:64–66.